Food Hydrocolloids 147 (2024) 109375

Contents lists available at ScienceDirect

Food Hydrocolloids

journal homepage: www.elsevier.com/locate/foodhyd

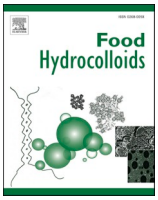

Hemp protein hydrolysates' ability to inhibit ice recrystallization is influenced by the dispersing medium and succinylation

Avery Ollis, Tong Wang, Vermont P. Dia *

Department of Food Science, The University of Tennessee Institute of Agriculture, 2510 River Dr, Knoxville, TN, 37996, USA

ARTICLE INFO

Keywords:
Hemp protein isolate
Ice recrystallization inhibition
Enzymatic hydrolysis
Succinylation
Splat assay
Medium effect

ABSTRACT

Freezing damage to foods can occur due to the formation of large ice crystals in the microstructure of foods, leading to unfavorable changes in the quality. The objective of this study was to determine the ice recrystallization inhibition (IRI) activity of hemp protein isolate (HPI) as affected by enzymatic hydrolysis and modification by succinylation. The IRI activity was evaluated using splat assay in phosphate buffer saline (PBS) and 10 mM NaCl. Enzymatic hydrolysis did not result in the production of IRI active hydrolysates when evaluated in PBS. Succinylation at 0.25:1 molar ratio of bromelain and trypsin hydrolysates resulted in the most IRI active hemp protein hydrolysates in PBS, having a 49% and 46% increase in IRI activity. When evaluated at 10 mM NaCl, both unmodified and modified HPI hydrolysates are IRI active. The unmodified hydrolysates were all significantly more IRI active in 10 mM NaCl, the hydrolysate produced by bromelain hydrolysis for 60 min had increased activity by 42% in the medium compared to PBS. Our results show that the ability of HPI hydrolysates to inhibit growth of ice crystal is influenced by the dispersing medium used during splat assay and succinylation.

1. Introduction

Freezing is a common preservation method in the food industry used to maintain the freshness of cellular foods like fruits, vegetables, and meats (Li et al., 2018). Although freezing slows enzymatic activity and inhibits microbial growth in foods, there are limitations to freezing that can negatively affect the quality of food products (Dalvi-Isfahan et al., 2019). One of these limitations is ice recrystallization. Ice recrystallization describes the change in ice size, shape, and number of ice crystals. More specifically, ice recrystallization is defined by the increase in ice crystal size and the decrease in the number of ice crystals in the system (Kawai & Hagiwara, 2018). Accretion, isomass rounding off, and Ostwald ripening are the different types of recrystallizations in ice. Accretion is the thermodynamically favorable process when ice crystals fuse (Buckley & Lillford, 2009). Isomass rounding off occurs after an increase in temperature, ice crystals melt or partially melt, and re-freeze into larger ice crystals (Buckley & Lillford, 2009). Ostwald ripening is the growth of large ice crystals at the expense of smaller ice crystals, a thermodynamically favorable process as well (Kawai & Hagiwara, 2018). The formation of large ice crystals physically damages the microstructure of cellular food products causing unfavorable changes in quality. After thawing, changes in color, flavor, and texture are common after freezing damage occurs (Xin et al., 2015).

One solution to this limitation is the use of antifreeze proteins (AFPs). AFPs were first discovered in the blood of Arctic fish and were later discovered in overwintering plants and insects (Gharib et al., 2022). Some AFPs have ice recrystallization inhibition (IRI) activity, the ability to inhibit the growth of large ice crystals during ice recrystallization (Gharib et al., 2022) giving potential for their use in cryopreservation. For instance, AFPs can offer ice cream a smooth texture (Munoz et al., 2017) and could enhance and improve the total gas and gassing rate in frozen dough (Liu et al., 2018). The proposed mechanism for this ability is through an ice-binding mechanism. Amphiphilic AFPs bind to the ice by hydrogen bonding while the hydrophobic domains of the protein repel water molecules preventing ice from continuing to form. This mechanism has been explained through molecular docking, but limitations do exist with direct experimental proof of this mechanism (Yang et al., 2022). Another potential mechanism is the ability of AFPs to both promote and depress ice nucleation (Liu et al., 2016). They reported depression of ice nucleation when the non-ice binding face of AFPs was exposed to liquid water while facilitation of ice nucleation was observed when the ice binding face of AFPs was exposed to liquid water, a phenomenon generally called Janus effect (Liu et al., 2016). The utilization of AFPs as IRI active materials in the preservation of frozen food

* Corresponding author. Department of Food Science, The University of Tennessee, 2510 River Dr, Knoxville, TN, 37996, USA.
E-mail address: vdia@utk.edu (V.P. Dia).

https://doi.org/10.1016/j.foodhyd.2023.109375
Received 29 June 2023; Received in revised form 28 September 2023; Accepted 29 September 2023
Available online 29 September 2023

quality is limited by their relatively high cost associated with their presence in relatively low concentration and the method of their isolation and purification. Hence, it is important to identify natural compounds in abundance that can mimic the IRI activity of AFPs. Protein hydrolysates can be a viable option as reported in the literature, where gelatin hydrolysates from fish and soy protein isolate have been shown to inhibit ice growth (Damodaran & Wang, 2017; Wan et al., 2022).

In this work, the potential IRI activity of hemp protein isolate (HPI) was studied. HPI is a mixture of proteins, some of which are highly hydrophobic associated with its high concentration of hydrophobic amino acids like leucine and valine (Malomo & Aluko, 2015). Because amphiphilic proteins have been shown to have IRI activity, HPI was modified by enzymatic hydrolysis and succinylation to potentially increase its amphiphilicity. IRI activity can be observed by the splat assay method (Knight et al., 1988) commonly performed by dispersing the compound in phosphate-buffered saline (PBS) solution. In addition, several studies have found differences in IRI activity when using different salts and salt concentrations during splat assay (Warren et al., 2022).

The objectives of this work were to evaluate the effect of enzymatic hydrolysis and succinylation on the IRI activity of HPI. In addition, the effect of dispersing medium (PBS and 10 mM NaCl) on the IRI activity of HPI hydrolysates was investigated. This work could provide insight into modifying plant-based proteins to increase antifreeze abilities and possibly provide a plant-based solution to freezing damage to foods.

2. Materials and method

2.1. Materials

The hempseed hearts used were from Foods to Live (Brooklyn, NY). The enzymes used for hydrolysis are Alcalase from *Bacillus licheniformis* (EMD Milipore Corp. Bilierica, MA), bromelain (MP Biomedicals, Solon, OH), and trypsin (Alfa Aesar, Ward Hill, MA). The molecular weight marker used for the SDS-PAGE is the Broad Multi Pre-Stained Protein Standard and the gel that was used for the SDS-PAGE was the SurePAGE, Bis-Tris gel (GenScript, Piscataway, NJ). All other chemicals were purchased from ThermoFisher (Waltham, MA) unless otherwise stated.

2.2. Preparation of hemp protein isolate and hydrolysates

Hemp protein isolate (HPI) was extracted from 150 g of defatted hempseed hearts in 1.35L of deionized water at pH 12 using 2 N NaOH for 90 min at room temperature with stirring. The mixture was centrifuged at 10,000×*g* at 4 °C for 15 min. The supernatant was collected, and the pH was adjusted to 5 with an HCl solution. The solution was centrifuged again, the precipitate was collected and washed with deionized water for 2–3 min and centrifuged. The washing process was repeated one more time, the precipitate was collected, and freeze-dried.

HPI was hydrolyzed for 30 and 60 min in a 10% suspension in water at a pH of 8 for trypsin and Alcalase and a pH of 6.5 for bromelain with a concentration of 1% of each enzyme relative to protein. The trypsin hydrolysis was done at 37 °C and Alcalase and bromelain at 55 °C. In addition, a two-enzyme hydrolysis of HPI was performed as: trypsin hydrolysis for 1 h followed by Alcalase hydrolysis for 30 min, and trypsin hydrolysis for 1 h followed by bromelain hydrolysis for 30 min using the same conditions as above. After the hydrolysis was completed, the samples were boiled for 10 min to inactivate the enzyme. The dispersion was cooled to room temperature and centrifuged at 10,000×*g* at 4 °C for 10 min to separate the supernatant from the precipitate and then the supernatant was freeze-dried and characterized.

2.3. Modification of the hemp protein hydrolysates with succinic anhydride

HPI and its hydrolysates were modified with succinic anhydride (SA). A leucine standard curve was used to determine the primary amine in the hydrolysates using the *o*-pthaldialdehyde (OPA) method. The modification of the hydrolysates by SA was done at 1:1, 0.5:1, and 0.25:1 molar ratios of SA and the primary amine of the hydrolysates. The amount of SA was calculated based on the primary amine present in 0.1 g of the sample. The modification reaction was completed at a concentration of 2% sample in 0.1 M ammonium bicarbonate buffer with a pH of 9.0. The reaction continued for 3 h at room temperature, and the pH was monitored to be between 8 and 9. The reaction was stopped by lowering the pH to 6.5 and boiled for 30 min to remove the ammonium bicarbonate buffer (Basak & Singhal, 2022; Yang et al., 2016).

2.4. Protein concentration measurement by Bradford assay

The protein concentration of the hydrolysates was determined using Bradford assay (Kruger, 1994). Approximately 1 mg of each sample in deionized water was vortexed for 1 h and centrifuged for at 10,000×*g* a 4 °C for 5 min. The supernatant was collected and diluted 10x with deionized water. One hundred μL of samples and standards ranging from 0 to 20 μg/mL were plated in a 96-well plate with 100 μL of the Bradford reagent (Alfa Aesar, Ward Hill, MA). The plate was incubated at room temperature for 5 min and the absorbance was read at 630 nm. The protein concentration was calculated using bovine serum albumin (BSA) as standard. The calculated protein concentration was used to approximate equal amount of protein loading for SDS-PAGE experiment described below.

2.5. Protein profile by SDS-PAGE

The molecular weight profile of the samples was evaluated by sodium dodecyl sulfate–polyacrylamide gel electrophoresis (SDS-PAGE). One hundred μL of the sample were mixed with 100 μL of Laemmli buffer containing 5% β-mercaptoethanol and boiled for 10 min. Approximately 25 μg of protein (as measured by Bradford assay) were loaded in the SurePAGE, Bis-Tris, 10x8 gel and 5 μL Broad Multi Pre-Stained Protein Standard (GenScript, Piscataway, NJ). The proteins were separated at 200 V for 35 min. The gel was stained with Coomassie blue G-250 (Bio-Rad, Hercules, CA) overnight with shaking and destained with deionized water until desired background clarity has been achieved while changing the water periodically.

2.6. Average molecular weight determination by SEC-HPLC

To analyze the molecular weight distribution of the hydrolysates, size-exclusion chromatography high-performance liquid chromatography (SEC-HPLC) was performed. Samples were prepared in HPLC-grade water at a concentration of 1 mg/mL and filtered using nylon membrane filters (GE Healthcare Life Sciences). They were then analyzed using the 1200 Agilent HPLC system (Agilent Technologies, Santa Clara, CA). The HPLC system has an autosampler (G1329A), quaternary pump (G1311A), vacuum degasser (G1322A), temperature-controlled column oven (G1316A), and diode array detector (G1315D). The column used was the BioSep-SEC-S2000 column (300 × 7.80 mm, Phenomenex, Torrance, CA). The flow rate used was 1 mL/min and the mobile phase was 45% aqueous acetonitrile containing 0.1% trifluoroacetic acid. The molecular weight of the samples was calculated using the standard curve made from the standards composed of albumin, aprotinin, glucagon, bradykinin, glutathione, and glycine. The linear regression equation ($R^2 = 0.98$) from the standards was used to calculate the molecular weight of each peak in the samples. The average molecular weight of each sample was calculated by taking the percent area for each peak and multiplying it by its corresponding molecular weight.

2.7. Degree of hydrolysis measurement by OPA assay

A portion of the sample from SEC-HPLC was used to measure the

degree of hydrolysis by OPA assay (Spellman et al., 2003). Ten μL of samples were plated in a 96-well plate in duplicate followed by the addition of 200 μL of freshly prepared OPA reagent. The OPA reagent is composed of 50% of 100 mM sodium tetraborate, 42.8% deionized water, 5% of 20% (w/v) SDS, 2% of 40 mg/mL OPA in methanol, and 0.2% β-mercaptoethanol. The absorbance was read at 340 nm after 5 min incubation at room temperature.

2.8. Surface hydrophobicity measurement by ANS assay

HPI and its hydrolysates were prepared in 1x PBS solution at a concentration of 5 mg/mL and were vortexed for 1 h. They were then centrifuged at 10,000×*g* at 4 °C for 30 min and the supernatant was transferred into new microcentrifuge tubes. Each sample went through a serial dilution in 1x PBS solution to the final concentrations of 0.5–0.016 mg/mL. A black 96-well plate was used for the analysis to which 200 μL of each diluted sample was plated in the wells followed by 20 μL of 8 mM 8-anilinonaphthalene-1-sulfonic acid (ANS) prepared in 1x PBS. The excitation and emission were measured at 390 nm and 480 nm, respectively, and the surface hydrophobicity was reported as the slope of the line by plotting the fluorescence intensity against the sample concentration (Nisov et al., 2020).

2.9. Degree of modification measurement by TNBS assay

The degree of modification of the modified HPI and HPI hydrolysates was measured by 2,4,6-trinitrobenzene sulfonic acid (TNBS) (Wan et al., 2018). The unmodified and modified HPI and hydrolysates were prepared at a concentration of 100 μg/mL in 0.1 M sodium bicarbonate at a pH of 8.5. The samples were vortexed for 1 h and centrifuged for 30 min at 10,000×*g* at 4 °C. The supernatant was transferred to a new microcentrifuge tube. Two hundred fifty μL of the 0.01% (w/v) TNBS solution was added to 500 μL of each sample. This mixture was incubated at 37 °C for 2 h, then the reaction was stopped by adding 250 μL 10% SDS and 125 μL 1 N HCl to each sample. The absorbance was read at 340 nm. The degree of modification was calculated by

$$D = ((U - M) / U)) \times 100 \quad (1)$$

where D is the degree of modification, U is the absorbance of the unmodified HPI and hydrolysates, and M is the absorbance for the modified HPI and hydrolysates (Shilpashree et al., 2015).

2.10. Determination of IRI activity by splat assay

The IRI activity of the samples was measured by splat assay using polarized light microscopy (Leica, DM2700M, Wetzlar Germany) (Knight et al., 1988). The cooling stage used was the HCS 302 (Insect instrument, Boulder, Colorado) and a digital camera (Leica, DMC4500, Wetzlar, Germany) was used on the microscope. The hydrolysates and polyethylene glycol (PEG) were solubilized in 1x PBS and 10 mM NaCl at a concentration of 2%. These samples were dropped from a syringe with a needle diameter of 0.90 mm from 1.5 m onto glass slides that were previously stored at −80 °C. Once the sample was dropped, it was placed into the microscope stage which was kept at a temperature of −8 °C. The image of ice crystals was captured after 30 min. Three pictures were taken randomly within the slide and a second analysis of the same sample was performed. The diameters of the ice crystals were calculated using Cellpose as previously reported (Saad et al., 2023). The diameters of the ice crystals were compared to the PEG sample as the negative control. The percent Feret's maximum diameter (%FD) relative to that of the PEG diameter was calculated. The lower the percentage the greater the IRI activity.

2.11. Statistical analysis

All experiments were completed in three replicates. The statistical analysis was done by SAS Institute Inc. (Cary, NC). The data were evaluated to determine significant differences using ANOVA with Tukey as the Posthoc test and correlation with a P-value of 0.05. Type III tests of fixed effects were done with ANOVA with Tukey as the Posthoc test.

3. Results and discussion

3.1. Characterization of hemp protein isolate and its enzymatic hydrolysates

3.1.1. Average molecular weight and protein profile

The average molecular weight of HPI and its hydrolysates by SEC-HPLC is shown in Table 1. The unhydrolyzed HPI had the highest average molecular weight at 50.6 ± 1.1 kDa. Enzymatic hydrolysis resulted in reduced average molecular weight. Trypsin, bromelain, and Alcalase hydrolysis for 1 h reduced average molecular weight to 4.8, 3.3, and 1.1 kDa, respectively. Trypsin hydrolysis for 1 h followed by bromelain and Alcalase hydrolysis for 30 min further reduced the average molecular weight to 1.7 and 2.5 kDa, respectively.

The average molecular weight of the unhydrolyzed HPI agrees with findings in literature because edestin has a molecular weight of about 20–35 kDa, with an albumin protein being detected at about 50 kDa (Sun et al., 2021). The differences in the average molecular weight of each hydrolysate can be attributed to the specificity of the enzymes used. Trypsin is highly specific as it cleaves only the carboxylic sides of lysine and arginine (Vandermarliere et al., 2013) Bromelain is less specific in hydrolyzing proteins than trypsin but more specific in comparison to Alcalase. Bromelain has specificity for cleaving peptide bonds of alanine, leucine, and glycine (de Lencastre et al., 2016), while Alcalase has a broad specificity endoprotease with a preference for hydrolyzing bonds containing aromatic amino acid residues (Damodaran & Parkin, 2017). The two-enzyme sequential hydrolysis was performed due to the trypsin hydrolysates having the highest average molecular weight of the hydrolysates. The sequential hydrolysis was done to observe possible differences in characteristics between the single hydrolysis treatment and the two-enzyme sequential treatment. The average molecular weight of these hydrolysates was lower when compared to the trypsin hydrolysate, which was expected due to additional enzymatic hydrolysis.

Similar results of the molecular weight profile of HPI and its

Table 1
Characterization of unmodified HPI and its hydrolysates.

Enzyme	Time (min)	Average MW (kDa)	Surface hydrophobicity	DH (%)
Unhydrolyzed		50.6 ± 1.1^{a}	68,866 ± 17,216^{a}	1.5 ± 0.8^{d}
Bromelain	30	3.3 ± 0.3^{bc}	7,498 ± 630^{b}	9.0 ± 1.6^{bcd}
	60	3.3 ± 0.1^{bc}	17,708 ± 439^{b}	6.8 ± 0.9^{cd}
Trypsin	30	5.1 ± 0.9^{b}	13,804 ± 2,375^{b}	5.6 ± 0.7^{cd}
	60	4.8 ± 1.3^{b}	12,710 ± 833^{b}	6.4 ± 0.9^{cd}
Alcalase	30	2.4 ± 0.4^{cd}	10,623 ± 2,757^{b}	16.2 ± 2.5^{b}
	60	1.1 ± 0.2^{d}	5,444 ± 536^{b}	33.0 ± 7.0^{a}
Trypsin & Bromelain	60 & 30	1.7 ± 0.0^{cd}	5,305 ± 703^{b}	34.5 ± 5.0^{a}
Trypsin & Alcalase	60 & 30	2.5 ± 0.1^{cd}	4,593 ± 733^{b}	10.6 ± 0.7^{bc}

Means followed by the same superscript letter within a column are not significantly different at a 5% level according to Tukey- Kramer HSD.

hydrolysates were found by SDS-PAGE shown in Fig. 1A. The unhydrolyzed hemp showed dark bands at just under the 30 kDa molecular weight marker and just over the 35 kDa marker. There is a faint band at the 50 kDa marker as well. Edestin is made up of six subunits with each of them having an acidic and basic subunit that are connected by disulfide bonds (Sun et al., 2021). Since the electrophoresis was conducted under reducing conditions by using beta-mercaptoethanol, the disulfide bonds in the protein are converted to thiol groups resulting in dissociation and denaturation of the protein (Sun et al., 2021). According to literature, the acidic subunit has a molecular weight of about 35 kDa and the basic subunit is about 20 kDa which agrees with our result for unhydrolyzed HPI as shown in Fig. 1A (Sun et al., 2021).

The SDS-PAGE confirms the results from the SEC-HPLC for the hydrolysates. The trypsin hydrolysates had bands at the 15 kDa molecular weight marker, this was the highest out of all the hydrolysates. This agrees with the SEC-HPLC data as those results found the trypsin hydrolysates to be the least hydrolyzed with the highest average molecular weight. The bromelain hydrolysates showed to have dark bands at the 5 kDa molecular weight marker and below the 15 kDa marker. These bands show that the bromelain hydrolysates had the second highest molecular weight after the trypsin hydrolysates. This agrees with the SEC-HPLC data as the average molecular weight for both is about 3.3 kDa. The Alcalase hydrolysates showed faint bands at the 5 kDa molecular weight marker, indicating that they were the most hydrolyzed with the lowest average molecular weight. The hydrolysates that were hydrolyzed by two enzymes showed faint bands at the 5 kDa marker. Fig. 1B shows the chromatogram from SEC-HPLC of the HPI hydrolysates comparing with unhydrolyzed HPI. This image shows the difference in the retention time of the peaks of the unhydrolyzed HPI and the hydrolysates. It can be observed that enzymatic hydrolysis shifted the chromatograms peaks to the right, confirming the conversion of high molecular weight proteins to low molecular peptides. The Alcalase and trypsin & Alcalase hydrolysates had the largest peaks at later retention times indicating that these hydrolysates have the lowest molecular weight. The bromelain hydrolysates had the second largest peaks at higher retention times followed by the trypsin hydrolysates. This confirms the findings of the SDS-PAGE and the calculated average molecular weight.

3.1.2. Degree of hydrolysis

After analyzing the average molecular weight, the degree of hydrolysis was done by the OPA assay to further characterize the hydrolysates and to confirm the level of hydrolysis. In Table 1, the Alcalase 60 min and the trypsin & bromelain hydrolysates had the highest degree of hydrolysis at 33.0% and 34.5%, respectively. The next hydrolysates with the highest degree of hydrolysis are the Alcalase 30 min and the trypsin & bromelain. The hydrolysates with the lowest degree of hydrolysis are the trypsin hydrolysates, followed by the bromelain hydrolysates having the second lowest degree of hydrolysis. From these results, it can be confirmed that the average molecular weight relates to the degree of hydrolysis. In terms of enzymes used, it can be concluded that the broad specificity of the Alcalase enzyme results in highly hydrolyzed hydrolysates (Damodaran & Parkin, 2017). As the enzyme becomes more specific, the degree of hydrolysis decreases, and the average molecular weight increases. Another trend that was observed was an increase in degree of hydrolysis with increasing hydrolysis time, apart from the bromelain hydrolysates. The bromelain 60 min hydrolysate had a lower degree of hydrolysis than the 30 min hydrolysate, this result was unexpected. This possibly could be explained by their similar average molecular weights and bromelain being a less specific enzyme. Another unexpected result was the low degree of hydrolysis of the trypsin & Alcalase hydrolysate compared to the trypsin & bromelain treated hydrolysate. The molecular weight of the trypsin & Alcalase hydrolysate was larger than the trypsin & bromelain, indicating it may have been less hydrolyzed.

3.1.3. Surface hydrophobicity

The surface hydrophobicity of the HPI and its hydrolysates was analyzed. This method allows the calculation of the hydrophobicity on the surface of a protein (Deshpande & Sathe, 2018). Surface hydrophobicity can help find possible correlations between the surface hydrophobicity of a protein and IRI activity as hydrophobicity and amphiphilicity have been found to be important factors contributing to IRI activity (Banach et al., 2018). From the data shown in Table 1, the unhydrolyzed HPI has the highest surface hydrophobicity, and this confirm the previous study reporting that HPI is highly hydrophobic (Malomo & Aluko, 2015). The trypsin hydrolysates had a surface hydrophobicity of 13,804 and 12,710. The bromelain hydrolysates had a surface hydrophobicity of 7,498 and 17,708. The Alcalase hydrolysates had lower surface hydrophobicity of about 10,623 and 5,444. The hydrolysates of the two enzyme treatments had the lowest surface hydrophobicity of 5,305 and 4,593. From these results the bromelain 60 min

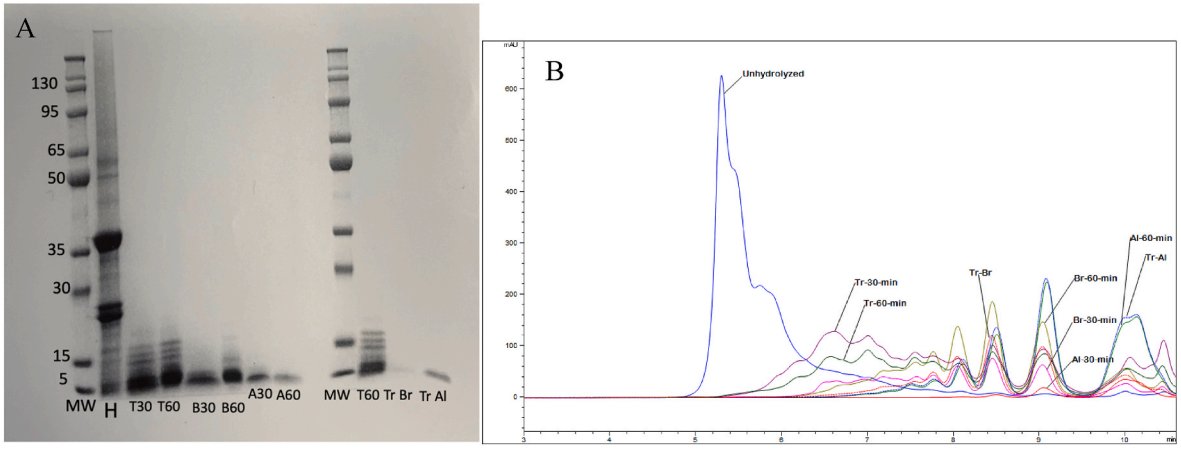

Fig. 1. Protein profile and molecular weight distribution of hemp protein isolate (HPI) and its hydrolysates. A) Electropherogram of HPI and its corresponding hydrolysates. The lane abbreviations: MW is the molecular weight marker, H is the unhydrolyzed HPI, T30 is the trypsin 30 min hydrolysate, T60 is the trypsin 60 min hydrolysate, B30 is the bromelain 30 min hydrolysate, B60 is the bromelain 60 min hydrolysate, A30 is the Alcalase 30 min hydrolysate, A60 is the Alcalase 60 min hydrolysate, Tr Br is the hydrolysate hydrolyzed by trypsin for 60 min and bromelain for 30 min, Tr Al is the hydrolysate hydrolyzed by trypsin for 60 min and Alcalase for 30 min. B) Overlaid chromatograms from SEC-HPLC of HPI and its hydrolysates. The peak labeled unhydrolyzed is the unhydrolyzed HPI, Al-60 is the Alcalase 60 min hydrolysate, Al-30 is the Alcalase 30 min hydrolysate, Br-30 is the bromelain 30 min hydrolysate, Br-60 is the bromelain 60 min hydrolysate, Tr-60 is the trypsin 60 min hydrolysate, Tr-30 is the trypsin 30 min hydrolysate, Tr-Br is the trypsin & bromelain hydrolysate, Tr-Al is the trypsin & Alcalase hydrolysate.

hydrolysis produced the most surface hydrophobic hydrolysates, the surface hydrophobicity of these hydrolysates increased with time. This trend was seen with the Alcalase hydrolysates, but it was not seen with the trypsin hydrolysates as the surface hydrophobicity of 30 min hydrolysates was similar to the 60 min hydrolysates. The two-enzyme treatment had similar surface hydrophobicity to the 60 min Alcalase hydrolysate. When comparing the surface hydrophobicity of the hydrolysates and the unhydrolyzed HPI, it can be concluded that the surface hydrophobicity decreased after enzymatic hydrolysis. Hydrolysis is a technique that is used to increase the solubility of proteins (García et al., 2013), hence enzymatic hydrolysis resulted in reduced surface hydrophobicity of HPI hydrolysates.

3.2. Characterization of succinic anhydride modified HPI and hydrolysates

To enhance the amphiphilicity of HPI and its hydrolysates, SA modification was conducted. Succinylation is a common reaction used to modify proteins. It is a nucleophilic substitution reaction that specifically attacks the ε-amino group of lysine and hydroxyl groups in proteins (Shilpashree et al., 2015). These groups are replaced with succinyl carboxyl groups forming an amide bond after the opening of the anhydride ring during the reaction. The added succinyl carboxyl groups increase the electronegativity of the protein resulting in increased water solubility and ability to carry ions (Mirmoghtadaie et al., 2009). Succinylation can change the structure of the proteins and their hydrolysates which can result in changes in their properties. The molecular weight of the 0.25:1 modified forms of the HPI and hydrolysates is shown in Table 2. Some of the modified proteins' MW slightly increased when compared to the unmodified hydrolysates. This is explained by the succinylation reaction which added hydrophilic groups to the hydrolysates, and a change in MW after succinylation has been seen in a past study as well (Mirmoghtadaie et al., 2009; Yang & Gibson, 2019). In general, succinylation resulted in a reduction in the surface hydrophobicity of HPI hydrolysates. This was expected due to HPI being a hydrophobic protein, and the purpose of the modification was to increase the hydrophilicity and decrease the hydrophobicity of the protein (Basak & Singhal, 2022). Table 2 also show that in general, the degree of modification increased as the molar ratio of SA to primary amines increased. The TNBS assay was used for degree of modification instead of the OPA assay because it has been used in previous studies for degree of succinylation (Sebii et al., 2021; Wan et al., 2018; Shilpashree et al., 2015).

3.3. IRI activity of hemp protein isolate and its enzymatic hydrolysates

To determine the IRI activity of HPI and its modified forms, a splat assay was conducted. The percent Feret's diameter (FD) relative to the same concentration of PEG of each sample of the HPI is shown in Fig. 2. FD is the maximum diameter in micrometers (μm) of the ice crystals after 30 min of annealing time. A percentage relative to the negative control, PEG, allows for the normalization of the FD values. Three replicates of each sample were done, and the average is shown in Fig. 2. The data show that the HPI did not have IRI activity when tested in PBS. The percent of FD out of PEG was over 100% for the HPI, meaning that the FD for these samples were all larger than the control. The lack of IRI activity could be explained by the hydrophobicity and the large and rigid structure of the HPI.

Because native HPI did not have IRI activity, the protein underwent enzymatic hydrolysis with bromelain, trypsin, and Alcalase. Enzymatic hydrolysis breaks down the protein through cleavage of peptide bonds, increasing the number of free amino acids and peptides (Xu et al., 2021). In addition, hydrolysis produces a product with higher solubility than the parent protein and will change their molecular weight distributions (Xu et al., 2021). Past studies have discovered a possible correlation between differences in molecular weight and IRI activity, depending on the protein (Leiter et al., 2016). Hence, enzymatic hydrolysis was done to observe any possible changes in IRI activity of HPI. The different enzymes were chosen based on their differences in specificity when cleaving peptide bonds. The hydrolysates' percent FD relative to PEG is also shown in Fig. 2. The hydrolysates did not show any IRI activity in PBS. The percent FD was over 100%, meaning that the FD was larger than the control for each hydrolysate. This lack of IRI activity could be due to the imbalance of hydrophobic and hydrophilic moiety in the

Table 2
Characterization of HPI and its hydrolysates modified at three levels of SA.

Modification	Enzyme	Time (min)	Average MW (kDa)	Surface hydrophobicity	Degree of SA Modification (%)
0.25:1	Unhydrolyzed	–	42.8 ± 8.1^{a}	$3{,}504 \pm 515^{ij}$	44.7 ± 1.5^{bcdef}
	Bromelain	30	4.6 ± 0.7^{b}	$8{,}532 \pm 436^{cde}$	30.1 ± 1.9^{efghi}
		60	3.9 ± 1.2^{b}	$14{,}017 \pm 564^{a}$	43.9 ± 6.0^{bcdef}
	Trypsin	30	4.8 ± 0.3^{b}	$5{,}283 \pm 1{,}378^{defghij}$	19.6 ± 0.4^{i}
		60	3.7 ± 1.0^{b}	$8{,}229 \pm 1{,}637^{cdefg}$	18.5 ± 3.6^{i}
	Alcalase	30	1.7 ± 0.4^{b}	$3{,}465 \pm 536^{ij}$	57.4 ± 3.8^{ab}
		60	2.4 ± 0.5^{b}	$3{,}463 \pm 1{,}719^{ij}$	57.4 ± 0.9^{ab}
	Trypsin & Bromelain	60 & 30	2.8 ± 0.4^{b}	$3{,}291 \pm 739^{j}$	20.4 ± 7.2^{hi}
	Trypsin & Alcalase	60 & 30	1.3 ± 0.0^{b}	$4{,}500 \pm 1{,}760^{ghij}$	67.6 ± 2.6^{a}
0.5:1	Unhydrolyzed	–	43.8 ± 0.6^{a}	$8{,}439 \pm 851^{cdef}$	49.0 ± 0.5^{bcd}
	Bromelain	30	1.8 ± 0.0^{b}	$7{,}188 \pm 910^{cdefghi}$	31.5 ± 6.2^{efghi}
		60	1.9 ± 0.0^{b}	$9{,}049 \pm 1{,}420^{bcd}$	25.7 ± 12.9^{ghi}
	Trypsin	30	4.6 ± 0.1^{b}	$10{,}769 \pm 851^{abc}$	21.9 ± 6.9^{hi}
		60	4.5 ± 0.4^{b}	$10{,}133 \pm 1{,}412^{bc}$	27.8 ± 6.9^{fghi}
	Alcalase	30	1.3 ± 0.2^{b}	$3{,}186 \pm 671^{j}$	37.0 ± 15.2^{defgh}
		60	1.4 ± 0.0^{b}	$1{,}888 \pm 236^{j}$	54.5 ± 1.1^{abc}
	Trypsin & Bromelain	60 & 30	1.6 ± 0.1^{b}	$3{,}909 \pm 596^{hij}$	34.7 ± 1.1^{defghi}
	Trypsin & Alcalase	60 & 30	1.1 ± 0.1^{b}	$4{,}509 \pm 779^{ghij}$	56.5 ± 1.4^{ab}
	Unhydrolyzed	–	41.2 ± 5.3^{a}	$12{,}520 \pm 3{,}556^{ab}$	45.3 ± 1.5^{bcde}
	Bromelain	30	4.0 ± 1.1^{b}	$4{,}025 \pm 826^{hij}$	39.0 ± 8.3^{cdefg}
		60	2.9 ± 1.9^{b}	$10{,}029 \pm 1{,}180^{bc}$	55.6 ± 5.9^{abc}
	Trypsin	30	5.3 ± 0.2^{b}	$4{,}914 \pm 831^{efghij}$	41.7 ± 3.6^{bcdefg}
		60	5.8 ± 0.7^{b}	$7{,}614 \pm 1{,}127^{cdefgh}$	46.6 ± 5.1^{bcde}
	Alcalase	30	1.5 ± 0.1^{b}	$3{,}590 \pm 679^{ij}$	68.1 ± 3.0^{a}
		60	1.3 ± 0.2^{b}	$3{,}217 \pm 673^{j}$	68.2 ± 0.5^{a}
	Trypsin & Bromelain	60 & 30	1.4 ± 0.0^{b}	$4{,}736 \pm 858^{fghij}$	34.7 ± 1.1^{defghi}
	Trypsin & Alcalase	60 & 30	1.1 ± 0.0^{b}	$2{,}405 \pm 496^{j}$	70.5 ± 1.2^{a}

Means followed by the same superscript letter within the same column are not significantly different at a 5% level according to Tukey- Kramer HSD.

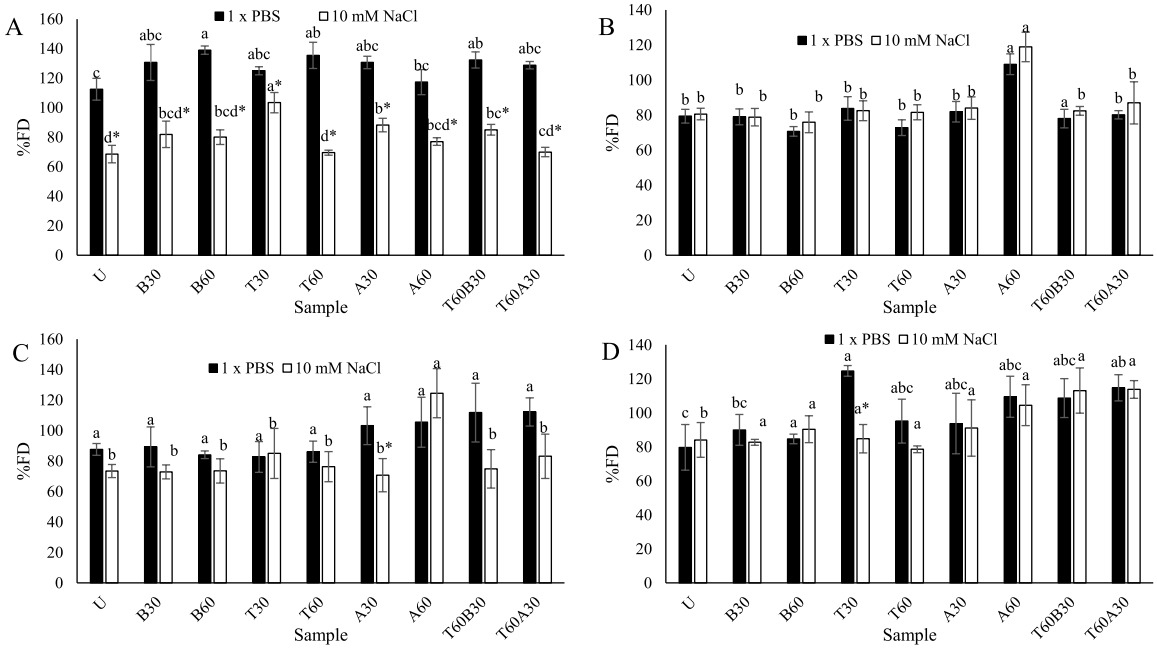

Fig. 2. Percent Feret's Diameter (FD, relative to PEG) of Unmodified and Modified HPI and Hydrolysates in Two Dispersing Media. A) Unmodified HPI, B) 0.25:1 modified HPI by succinylation, C) 0.5:1 modified HPI by succinylation, and D) 1:1 modified HPI by succinylation. Lowercase letters indicate the significance among samples in the same dispersing media (either 1 x PBS or 10 mM NaCl). Asterisk (*) following lowercase letter means significant difference between the dispersing media.

hydrolysates (Biggs et al., 2019). Fig. 3A and B show that there is no significant correlation between molecular weight and IRI activity of HPI hydrolysates when tested in either PBS or 10 mM NaCl.

As the solubility and structure of proteins and protein hydrolysates can be affected by salt concentration, we tested the IRI activity of HPI and its hydrolysates in 10 mM NaCl at pH 7.0. Previous studies have shown that salt and buffer conditions can affect IRI activity (Warren et al., 2022). As shown in Fig. 2, the unmodified hydrolysates were each significantly more IRI active in the 10 mM NaCl solution than in the PBS solution. The enhanced IRI activity observed in lower salt system can be explained by an increase crowding of molecules as the amount of unfrozen water at −8 °C is lower in 10 mM NaCl than in 1 x PBS dispersing medium. Also, it can be explained by the "salting-in" theory of the low concentration of salt increasing the solubility of the protein and allowing it to be completely dispersed to the solution. The protein surface area available to absorb into the ice/water interface is increased, therefore increasing antifreeze activity (Evans et al., 2007; Kiran-Yildirim & Gaukel, 2020; Kristiansen et al., 2008). It could also be due to a decrease

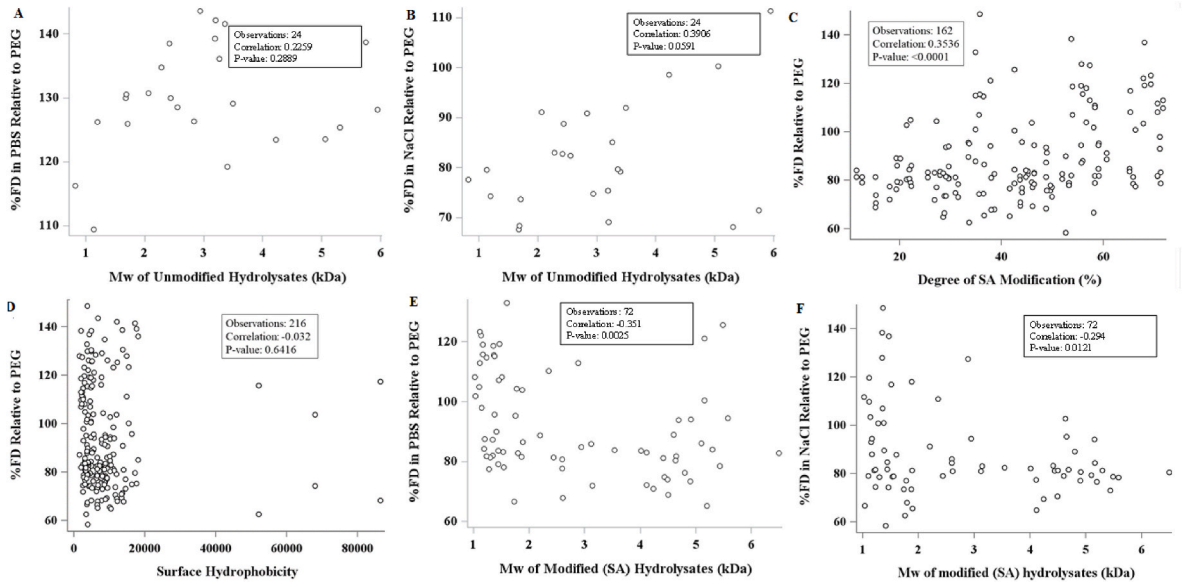

Fig. 3. Relationship between IRI activity and molecular characteristics of HPI hydrolysates and their succinylated forms. A) No significant correlation between % Feret's Diameter (%FD) and molecular weight (Mw) of unmodified HPI hydrolysates in PBS. B) No significant correlation between (%FD) and Mw of unmodified HPI hydrolysates in 10 mM NaCl. C) Significant correlation between %FD and degree of SA modification (%) of HPI hydrolysates. D) No significant correlation between % FD and surface hydrophobicity of HPI and hydrolysates. E) Significant negative correlation between %FD and Mw of SA modified HPI and hydrolysates in PBS. F) Significant negative correlation between %FD and Mw of SA modified HPI and hydrolysates in 10 mM NaCl.

in ion shielding, compared to the samples in PBS, which can change the interaction of the molecules at the ice/water interface (Wang et al., 2022). Another potential explanation on the effect of dispersing medium on the IRI activity of HPI hydrolysates is ion composition and concentration. For instance, Wu et al. (2017) reported that the mean ice crystal size can be affected by changing the anions in the initial solution. They also showed the effect of different anions (using Na^+ as the cation) and cations (using Cl^- as the anion) on mean ice grain size indicating that Hofmeister series influences ice recrystallization (He et al., 2018; Wu et al., 2017). Representative ice crystal images of tests run in 10 mM NaCl can be seen in Supplementary Fig. 1.

3.4. Effects of succinylation on the IRI activity of HPI and hydrolysates

The IRI activity of the modified hydrolysates was investigated by splat assay and is shown in Fig. 2B–D. In PBS, the 0.25:1 modified hydrolysates are significantly more IRI active than the unmodified hydrolysates, except for the Alcalase 60 min hydrolysate. Representative ice crystal images of 0.25:1 modified hydrolysates can be seen in Supplementary Fig. 2. The 0.5:1 modification lowered the % FD, however only the trypsin hydrolysates were significantly more IRI active after modification at 0.5:1. Within this modification, the Alcalase 30 min hydrolysate was significantly more active in 10 mM NaCl. The 1:1 modification significantly increased the IRI activity of the HPI and hydrolysates except for the trypsin 30 min, Alcalase 60 min, and double enzyme treated hydrolysates. The trypsin 30 min hydrolysate in the 1:1 modification was significantly more IRI active in the 10 mM NaCl. Table 3 shows the type III tests of fixed effects of the % FD of unmodified and modified. This table confirms there is a significant difference between the different modification levels, enzymes, and the dispersing medium. It also shows that the interaction of the different enzymes and the modification levels caused significant changes in the IRI activity of the hydrolysates, as well as the interactions between the modification levels and dispersing medium and all three factors of the enzymes, modification levels, and the medium. The type III fixed effects from statistical analysis by Tukey's in Table 4, shows a significant difference in the IRI activity of 0.25:1 and unmodified hydrolysates and between the 0.5:1 and 1:1 modification. The increase in IRI activity after modification can be explained by the reaction of succinylation when carboxyl groups attach to the protein, creating a more negative charge (Basak & Singhal, 2022). The increase in negative charge can increase the amphiphilicity of the hydrolysates, which is known to be an important factor in the mechanism of IRI activity (Basak & Singhal, 2022; Yang et al., 2022). Previous studies reported that these amphiphilic-modified forms of the hydrolysate's hydrogen bond to the ice with their hydrophilic domains, while the hydrophobic domains repel water molecules and prevent ice from continuing to grow (Yang et al., 2022).

From these results, it can be inferred that a lower molar ratio of SA used in modification provides a more favorable balance of hydrophilicity and hydrophobicity of the proteins. Fig. 3C supports this as it shows a significant positive correlation between % FD and degree of modification. The lower the level of modification, the smaller the % FD is, indicating a stronger IRI activity. The balance of hydrophilicity and hydrophobicity needed for IRI activity is supported by Fig. 3D. This figure shows no significant correlation between % FD and surface hydrophobicity. Increased surface hydrophobicity of the hydrolysates did not correlate with higher IRI activity, and that also applies to decreased hydrophobicity. This suggests there should be a balance of both characteristics for increased IRI activity. We also looked at the possible correlation of modified HPI hydrolysates molecular weight and their corresponding IRI activity. As shown in Fig. 3E and F, a negative weak correlation exists between the molecular weight of the modified HPI hydrolysates and their % FD when tested in both PBS and 10 mM NaCl, respectively. The modified hydrolysates with larger molecular weights had lower % FD and higher IRI activity. The hydrolysates with larger average molecular weights in this case are the trypsin and bromelain hydrolysates as previously discussed. It has been noted in other reports that the molecular weight of antifreeze proteins may influence their IRI activity (Congdon et al., 2013). Other studies in literature support the finding that a higher molecular weight yields more IRI activity (Congdon et al., 2013). IRI activity is affected by many factors, such primary and secondary structure, size, and the balance of hydrophilicity and hydrophobicity of the molecules, and this work provides such evidence. However, mechanistically how on the molecular level the samples influence ice crystal growth is still an unanswered question. Using pure compounds, applying precise and controlled structural modification, and more quantitative and deeper characterization of the molecular features at the water-ice interface can help understand the mechanism of action.

Table 3
Type III tests of fixed effects of %FD of unmodified and modified hydrolysates.

Effect	P-value
Enzyme	<0.0001
Modification	<0.0001
Enzyme * Modification	<0.0001
Dispersing media	<0.0001
Enzyme * Dispersing media	0.0772
Modification * Dispersing media	<0.0001
Enzyme * Modification * Dispersing media	<0.0001

Interaction values were found by Tukey- Kramer HSD with a 5% significance level.

Table 4
Type III tests of fixed effects of degree of SA modification on %FD.

Modification	Effect	P-value
None and 0.25:1	Enzyme	<0.0001
	Modification	<0.0001
	Enzyme * Modification	<0.0001
	Dispersing media	<0.0001
	Enzyme * Dispersing media	0.0043
	Modification * Dispersing media	<0.0001
	Enzyme * Modification * Dispersing media	<0.0001
0.5:1 and 1:1	Enzyme	<0.0001
	Modification	0.0008
	Enzyme * Modification	0.1192
	Dispersing media	<0.0001
	Enzyme * Dispersing media	0.1727
	Modification * Dispersing media	0.0987
	Enzyme * Modification * Dispersing media	0.0009

Interaction values were found by Tukey- Kramer HSD with a 5% significance level.

4. Conclusion

In conclusion, the unmodified HPI and hydrolysates are not IRI active in PBS. The IRI activity of the SA-modified HPI, and hydrolysates increased with a decreased level of modification, with the 0.25:1 modification being the most IRI active. The unmodified HPI and hydrolysates had some increased IRI activity in 10 mM NaCl than in PBS. Our results showed for the first time the ability of HPI hydrolysates and their succinylated forms to inhibit ice crystal growth.

CRediT authorship contribution statement

Avery Ollis: Conceptualization, Investigation, Formal analysis, Writing – original draft. Tong Wang: Conceptualization, Resources, Writing – review & editing, Funding acquisition. Vermont P. Dia: Conceptualization, Resources, Supervision, Writing – review & editing, Funding acquisition.

Declaration of competing interest

The authors declare that they have no conflict of interests.

Data availability

Data will be made available on request.

Acknowledgements

This study was supported by the National Science Foundation through funding (award number 2103558).

Appendix A. Supplementary data

Supplementary data to this article can be found online at https://doi.org/10.1016/j.foodhyd.2023.109375.

References

Banach, Konieczny, L., & Roterman, I. (2018). Why do antifreeze proteins require a solenoid? *Biochimie, 144*, 74–84.
Basak, S., & Singhal, R. S. (2022). Succinylation of food proteins- a concise review. *Lwt, 154*.
Biggs, Stubbs, C., Graham, B., Fayter, A. E. R., Hasan, M., & Gibson, M. I. (2019). Mimicking the ice recrystallization activity of biological antifreezes. When is a new polymer "active". *Macromolecular Bioscience, 19*(7), Article e1900082. n/a.
Buckley, S. L., & Lillford, P. J. (2009). Antifreeze proteins: Their structure, binding and use. In S. Kasapis, I. T. Norton, & J. B. Ubbink (Eds.), *Modern biopolymer science* (pp. 93–128). London: Elsevier.
Congdon, Notman, R., & Gibson, M. I. (2013). Antifreeze (Glyco)protein mimetic behavior of poly(vinyl alcohol): Detailed structure ice recrystallization inhibition activity study. *Biomacromolecules, 14*(5), 1578–1586.
Dalvi-Isfahan, Jha, P. K., Tavakoli, J., Daraei-Garmakhany, A., Xanthakis, E., & Le-Bail, A. (2019). Review on identification, underlying mechanisms and evaluation of freezing damage. *Journal of Food Engineering, 255*, 50–60.
Damodaran, S., & Parkin, K. L. (Eds.). (2017). *Fennema's food chemistry* (5th ed.). CRC Press.
Damodaran, & Wang, S. (2017). Ice crystal growth inhibition by peptides from fish gelatin hydrolysate. *Food Hydrocolloids, 70*, 46–56.
Deshpande, & Sathe, S. K. (2018). Interactions with 8-Anilinonaphthalene-1-sulfonic acid (ANS) and surface hydrophobicity of black gram (vigna mungo) phaseolin. *Journal of Food Science, 83*(7), 1847–1855.
Evans, Hobbs, R. S., Goddard, S. V., & Fletcher, G. L. (2007). The importance of dissolved salts to the in vivo efficacy of antifreeze proteins. *Comparative Biochemistry and Physiology Part A: Molecular & Integrative Physiology, 148*(3), 556–561.
García, Puchalska, P., Esteve, C., & Marina, M. L. (2013). Vegetable foods: A cheap source of proteins and peptides with antihypertensive, antioxidant, and other less occurrence bioactivities. *Talanta, 106*, 328–349.
Gharib, Saeidiharzand, S., Sadaghiani, A. K., & Koşar, A. (2022). Antifreeze proteins: A tale of evolution from origin to energy applications. *Frontiers in Bioengineering and Biotechnology, 9*, Article 770588, 770588.
He, Z., Liu, K., & Wang, J. (2018). Bioinspired materials for controlling ice nucleation, growth, and recrystallization. *Accounts of Chemical Research, 51*(5), 1082–1091.
Kawai, & Hagiwara, T. (2018). Control of physical changes in food products. *Advances in Experimental Medicine and Biology, 1081*, 385–399.
Kiran-Yildirim, & Gaukel, V. (2020). Thermal hysteresis and bursting rate in sucrose solutions with antifreeze proteins. *Chemical Engineering & Technology, 43*(7), 1383–1392.
Knight, Hallett, J., & DeVries, A. L. (1988). Solute effects on ice recrystallization: An assessment technique. *Cryobiology, 25*(1), 55–60.
Kristiansen, Pedersen, S. A., & Zachariassen, K. E. (2008). Salt-induced enhancement of antifreeze protein activity: A salting-out effect. *Cryobiology, 57*(2), 122–129.
Kruger. (1994). The Bradford method for protein quantitation. *Basic Protein and Peptide Protocols, 32*, 9–15.
Leiter, Mailänder, J., Wefers, D., Bunzel, M., & Gaukel, V. (2016). Influence of acid hydrolysis and dialysis of κ-carrageenan on its ice recrystallization inhibition activity. *Journal of Food Engineering, 209*, 26–35.
de Lencastre Novaes, Jozala, A. F., Lopes, A. M., de Carvalho Santos-Ebinuma, V., Mazzola, P. G., & Pessoa Junior, A. (2016). Stability, purification, and applications of bromelain: A review. *Biotechnology Progress, 32*(1), 5–13.
Liu, M., Liang, Y., Zhang, H., Wu, G., Wang, L., & Qian, H. (2018). Production of a recombinant carrot antifreeze protein by *Pichia pastoris* GS115 and its cryoprotective effects on frozed dough properties and bread quality. *Food Science & Technology, 96*, 543–550.
Liu, K., Wang, C., Ma, J., Shi, G., Yao, X., Fang, H., Song, Y., & Wang, J. (2016). Janus effect of antifreeze proteins on ice nucleation. *Proceedings of the National Academy of Sciences, 113*(51), 14739–14744.
Li, Zhu, Z., & Sun, D.-W. (2018). Effects of freezing on cell structure of fresh cellular food materials: A review. *Trends in Food Science & Technology, 75*, 46–55. https://doi.org/10.1016/j.tifs.2018.02.019
Malomo, & Aluko, R. E. (2015). A comparative study of the structural and functional properties of isolated hemp seed (Cannabis sativa L.) albumin and globulin fractions. *Food Hydrocolloids, 43*, 743–752. https://doi.org/10.1016/j.foodhyd.2014.08.001
Mirmoghtadaie, Kadivar, M., & Shahedi, M. (2009). Effects of succinylation and deamidation on functional properties of oat protein isolate. *Food Chemistry, 114*(1), 127–131.
Munoz, P., Marquez, S. L., & Gonzalez, F. D. (2017). Structure and application of antifreeze proteins from Antartic bacteria. *Microbial Cell Factories, 16*, 138–150.
Nisov, Ercili-Cura, D., & Nordlund, E. (2020). Limited hydrolysis of rice endosperm protein for improved techno-functional properties. *Food Chemistry, 302*, Article 125274, 125274.
Saad, Fomich, M., Día, V. P., & Wang, T. (2023). A novel automated protocol for ice crystal segmentation analysis using Cellpose and Fiji. *Cryobiology, 111*, 1–8.
Sebii, Karra, S., Bchir, B., Nhouchi, Z., Ghribi, A. M., Karoui, R., Blecker, C., & Besbes, S. (2021). Effect of succinylation on the secondary structures, surface, and thermal properties of date palm pollen protein concentrate. *Journal of Food Science and Technology, 58*(2), 632–640.
Shilpashree, Arora, S., Chawla, P., & Tomar, S. K. (2015). Effect of succinylation on physicochemical and functional properties of milk protein concentrate. *Food Research International, 72*, 223–230.
Spellman, McEvoy, E., O'Cuinn, G., & FitzGerald, R. J. (2003). Proteinase and exopeptidase hydrolysis of whey protein: Comparison of the TNBS, OPA and pH stat methods for quantification of degree of hydrolysis. *International Dairy Journal, 13*(6), 447–453.
Sun, X., Sun, Y., Li, Y., Wu, Q., & Wang, L. (2021). Identification and characterization of the seed storage proteins and related genes of Cannabis Sativa L. *Frontiers in Nutrition, 8*.
Vandermarliere, Mueller, M., & Martens, L. (2013). Getting intimate with trypsin, the leading protease in proteomics. *Mass Spectrometry Reviews, 32*(6), 453–465.
Wan, Z., Fei, T., & Wang, T. (2022). Inhibition of ice crystal growth by protein hydrolysates from different plant- and animal-based proteins. *Food Materials Research, 2*, 17.
Wang, Li, J., Zhou, J., Song, M., Wang, J., Li, X., Tang, C.-C., Lu, M., & Gu, R. (2022). The effect of ion environment changes on retention protein behavior during whey ultrafiltration process. *Food Chemistry X, 15*, Article 100393. https://doi.org/10.1016/j.fochx.2022.100393, 100393.
Wan, Liu, J., & Guo, S. (2018). Effects of succinylation on the structure and thermal aggregation of soy protein isolate. *Food Chemistry, 245*, 542–550.
Warren, M. T., Galpin, I., Bachtiger, F., Gibson, M. I., & Sosso, G. C. (2022). Ice recrystallization inhibition by amino acids: The curious case of alpha- and beta-alanine. *Journal of Physical Chemistry Letters, 13*.
Wu, S., Zhu, C., He, Z., Xue, H., Fan, Q., Song, Y., Francisco, J. S., Zeng, X. C., & Wang, J. (2017). Ion-specific ice recrystallization provides a facile approach for the fabrication of porous materials. *Nature Communications, 8*(1), Article 15154.
Xin, Zhang, M., Xu, B., Adhikari, B., & Sun, J. (2015). Research trends in selected blanching pretreatments and quick freezing technologies as applied in fruits and vegetables: A review. *International Journal of Refrigeration, 57*, 11–25.
Xu, Wen, Q.-H., Wang, R., Li, J., Chen, B.-R., & Zeng, X.-A. (2021). Enhanced synthesis of succinylated whey protein isolate by pulsed electric field pretreatment. *Food Chemistry, 363*, Article 129892, 129892.
Yang, & Gibson, G. E. (2019). Succinylation links metabolism to protein functions. *Neurochemical Research, 44*(10), 2346–2359.
Yang, Jiang, W., Chen, X., Chen, X., Wu, J., Huang, J., Cai, X., & Wang, S. (2022). Identification of novel antifreeze peptides from Takifugu obscurus skin and molecular mechanism in inhibiting ice crystal growth. *Journal of Agricultural and Food Chemistry, 70*(44), 14148–14156.
Yang, Yang, J., Zhang, Y., & Zhang, W. (2016). Influence of succinylation on physicochemical property of yak casein micelles. *Food Chemistry, 190*, 836–842.